UNIVERSITAT POLITÈCNICA
DE CATALUNYA
BARCELONATECH

Programa de Doctorat en Enginyeria Biomèdica
Departament d'Enginyeria de Sistemes,
Automàtica i Informàtica Industrial
Centre de Recerca en Enginyeria Biomèdica

Tesis Doctoral por compendio de publicaciones

Muscular pattern based on multichanel surface EMG during voluntary contractions of the upper-limb

Mislav Jordanić

September 2017

Directores:
Miguel Angel Mañanas Villanueva
Mónica Rojas-Martínez

Abstract

Extraction of neuromuscular information is an important and extensively researched issue in biomedical engineering. Information on muscle control can be used in numerous human-machine interfaces and control applications, including rehabilitation engineering, e.g., prosthetics, exoskeletons and rehabilitation robots.

Neuromuscular information can be extracted at the brain level, peripheral nerves, or muscles. Among these options, muscle interface is the only viable way of information extraction in everyday life. Although brain and nerve recordings are promising, they usually require invasive measurement and achieve relatively low extraction speed which prevents real time control. Even though in electromyographic (EMG) recordings information is not obtained directly from neural cells, it contains similar information as nerve recording. Information contained in action potential of the innervated muscle fibers (MUAP) is equivalent to the information contained in the action potential of corresponding motor neurons. Moreover, muscles contain multiple motor units that activate simultaneously so their electrical activity sums on the surface of the skin, resulting in a relatively high amplitude compared to the other bioelectrical signals. Therefore, due to the richness of neural information, noninvasiveness and high signal-to-noise ratio, the surface EMG is extensively used for man–machine interfacing, especially in commercial/clinical upper-limb prosthetic control.

Motivation and usefulness of this thesis lies in the fact that information associated with muscular pattern during exercises can be very useful in different applications such as monitoring patients' control strategies during recovery, personalizing rehabilitation processes to increase their effectiveness or to provide information to be used for control of external devices (EMG based control of prosthesis or exoskeletons).

Within this doctorate a pattern recognition approach was used to assess neuromuscular information and to identify subjects' intended motion based on multichannel surface electromyographic recordings. Research was focused on control strategies of upper-limb, both in normal subjects and in patients with impaired mobility caused by incomplete spinal cord injury. Methods which are proposed can be used for the design and monitoring of rehabilitation therapies intended for patients with neuromuscular impairment, as well for the control of external devices like rehabilitation robots, exoskeletons, prostheses and even virtual games. However, that is in the domain of future applications of this work and is not the scope of the thesis.

Contents

List of Tables

List of Figures

Chapter 1

Introduction

1.1 Muscle physiology

Movement is achieved by using over 600 skeletal muscles. Besides skeletal muscles, there are two other muscle types: smooth muscle, of which internal organs are mostly built, and cardiac muscle, building the heart. Only the skeletal muscles can be controlled voluntary.

Elementary building block of a muscle is muscle cell, or muscle fiber - *myocyte*. Myocytes are ensheated by *endomysium*, a connective tissue that contains nerves and capillaries. They are organized in bundles of 10 to 100 fibers, which are called *fascicles*, and surrounded by sheath of connective tissue, *perymisium*. Group of fascicles is finally grouped together and enveloped by *epimysium*, forming a muscle.

Sarcolema is the cell membrane of myocyte, consisting of a lipid bilayer that contains intracelular liquid, *myoplasma*. In the myoplasma, thin and thick filaments are serially connected, forming *sarcomeres*, which are longitudinally connected in *myofibrils* that extend through entire length of the myocyte. During shortening of muscle fibers, thin and thick filaments of sarcomeres are pulled together by cross-bridges between them. Total shortening of myofibril is summation of shortenings of sarcomeres of which it is composed.

During the stable state when there are no stimuli, i.e., in the resting state, the inside of the myocyte is at greater potential that the outside. This difference in potential is usually around 80

mV and it is caused by the higher concentration of positive ions, namely Na+ and K+, outside of the sarcolema (Nazmi et al., 2016).

Motor neurons transfer nerve impulses that control the muscle from spinal cord to neuromuscular junction. At the nerve endings action potentials trigger opens calcium channels, which enables calcium to enter axon terminals and trigger the release of the neurotransmitter *acetylcholine*. It is released to the narrow space between the axon and sarcolema, and causes sodium channels in sarcolema to open. Na+ ions now flow into the myoplasma by diffusion due to higher concentration of Na+ ions outside of the membrane. This process causes depolarization of sarcolema during which the outside potential of the muscle cell is at lower voltage than inside potential by around 30 mV. Depolarization is immediatelly followed by repolarization, a process during which the electrochemical balance and the resting potential of the cell are restored. It is achieved by flushing the Na+ ions outside of the sarcolema by the *ion pump*. The process can be seen in figures 1.1 and 1.2.

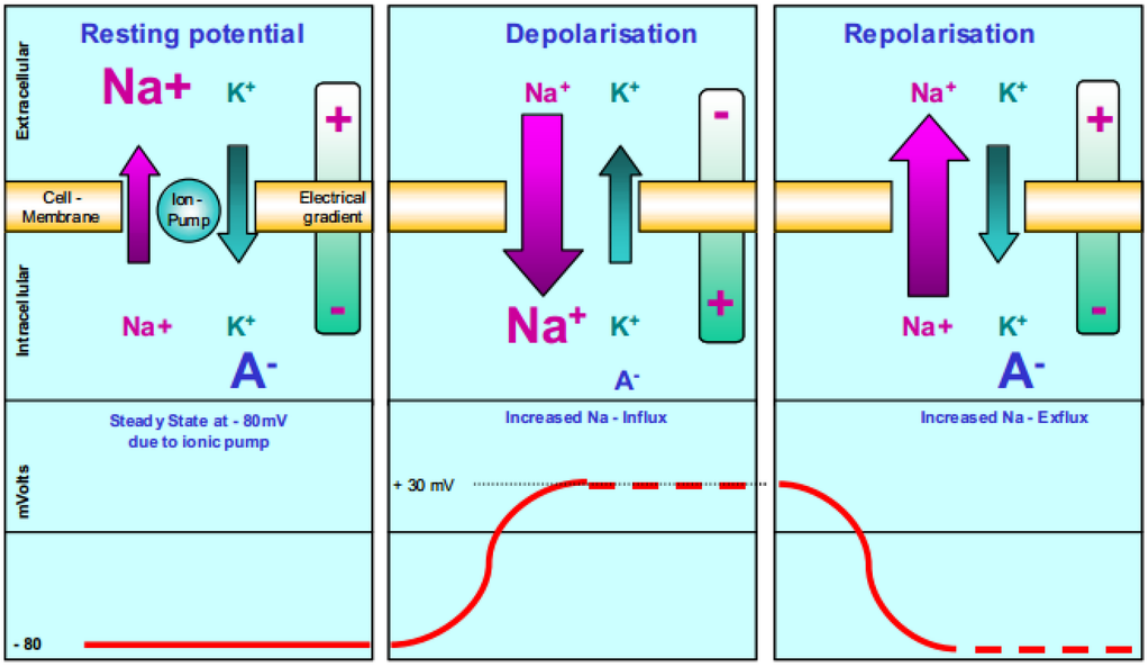

Figure 1.1: Ilustration of depolarization/repolarization of the muscle fiber. Adopted from (Nazmi et al., 2016)

If the amount of acetylcoline is sufficient for the excitation, depolarization/repolarization wave, that is, action potential, propagates longitudinally from the junction towards the ends of the fiber causing contraction (Henneberg, 1999). Speed of action potential propagation is called

conduction velocity and typically ranges around 4 m/s.

Detailed analysis of muscle physiology can be found elsewhere (Squire, 1986).

1.2 Muscle activation

Each motor neuron at the neuromuscular junction innervates several muscle fibers, forming the smallest functional unit called *motor unit*. It was firstly defined by Liddell and Sherrington in 1925 (Liddell and Sherrington, 1925; Sherrington, 1925) and is composed of motor neuron with axon and dendrites, and muscle fibers that axon innervates (Duchateau and Enoka, 2011). Since motor neuron with a single action potential usually evokes action potentials simultaneously in all belonging muscle fibers, by observing action potentials of the muscle fibers, information on activity of motor neurons in spinal cord or brain stem can be inferred (Merletti and Farina, 2016).

Pool of motor neurons that innervates entire muscle generally ranges from ten to thousand, depending on the muscle. (Merletti and Farina, 2016).

By the characteristics of muscle fiber, there are three main types of muscle fibers:

- Fast twitch, fatigable fibers (FF, or type IIb)
  They have high levels of ATP for anaerobic energy supply. They are present in pale muscles. glycolytic and work well in ischemic or low oxygen conditions. fast twitch, large forces. high nerve conduction velocity.

- Fast twitch, fatigue-resistant (FR, or type IIa) oxidative glycolytic, have fast twitch and are resistant to fatigue. intermediate conduction velocity

- Slow twitch, very resistant to fatigue (S, or type I) Oxidative and do not work well in low oxygen conditions. They generate small forces, have slow twitch and resistant to fatigue. lower nerve conduction velocity. This fiber type is very resilient to fatigue because of high oxidative metabolism and energy efficiency. They are present in high percentage in red muscles, such as soleus.

Muscle fibers innervated by the same motor neuron have similar histochemical and contractile characteristics.

Force that muscle fibers generate depends on firing frequency of the action potentials (rate coding) innervating the neuromuscular junction, and the recruitment strategy by which the motor units are activated, i.e., the number of activated motor units. Firing frequency and the recruitment strategy depend on the speed and force of contraction. Muscle units with low threshold are activated firstly, resulting in low force and high endurance, i.e., resistance to fatigue. If greater force is required, muscle units with higher threshold that are prone to fatigue are activated (Freund et al., 1975; Merletti and Parker, 2004). This was first proposed by Henneman et al. in 1965 (Henneman et al., 1965), who state that order of recruitment of motor neurons is based on size principle, that is, neurons with smaller axons are recruited at lower effort levels and with increase in force, larger motoneurons are recruited. Therefore, S type muscle units, which have the smallest motoneurons are recruited first, followed by FR type units, and finally FF units. The recruitment strategy can be seen in figure 1.3, whereas resistance to fatigue can be seen in figure 1.4.

1.3 Muscle fatigue

Muscle during contraction develops muscle fatigue. It is characterized by decrease of conduction velocity **Wdimaier**. Although muscle fatigue begins to develop at the beginning of contractions, it is a challenge to grade it during contraction. What

1.4 Surface electromyography

Muscle unit action potentnial (MUAP) is the combination of action potentials generated by the single motor unit. Myoelectric signal is a superposition of electrical activity (propagating action potentials) produced by the muscle fibers while contracting. It can be characterized (Farina et al., 2014)

EMG signals could be recorded either non-invasively (surface EMG, sEMG) or invasively with

needle and wire electrodes (intramuscular EMG, iEMG) (Marateb et al., 1999). Although iEMG signal is usually with higher quality (in terms of signal-to-noise ratio), it was shown that both approaches provide a similar quality of identification of upper-arm motor task(Hargrove et al., 2007).

Surface electromyographic signal (sEMG) is the sum of the electrical activity of the muscle fibers recorded on the surface of the skin. Since muscle fibers are activated by the impulse train of the innervating motor neurons, i.e. neural drive to the muscle, sEMG is the convolution of motor neuron spike trains by the motor unit action potential recorded on the electrodes (Farina et al., 2010, 2014).

$$sEMG(t) = \sum_{i=1}^{M} \sum_{j=-\infty}^{+\infty} MUAP_i(t)\ \delta(t - t_{i,j}) \tag{1.1}$$

, where M is the number of active motor units, $MUAP_i(t)$ is the action potential waveform of the i^{th} motor unit recorded by the electrodes, and $t_{i,j}$ is the time of the discharge of the i^{th} motor neuron. This model assumes there is no interference and that neuromuscular junction never fails, which is not the case. In the equation, $MUAP_i(t)$ is related to the electrophysiological state of the muscle fiber membranes, whereas neural information is contained in motor neuron spike trains $\delta(t - t_{i,j})$ citiraj The extraction of neural strategies from the surface EMG: an update.

Depending on number of electrodes used for the recording. the following classification exists: monopolar, bipolar, linear electrode array, and high-density EMG (see Figure 1.5)

HD-EMG 1.6

Technological advancement of EMG acquisition systems enables use of high-density electromyography (HD-EMG) **Surface EMG: how far can you go**. Using an array of closely spaced electrodes organized in a quadrature grid, a wide muscle area is recorded. This technology is the only one that allows insights into spatial distribution of motor units in a muscle. By observing the amplitude or intensity of signals recorded in different channels, it is possible to analyze how different muscle regions activate depending on joint position (Vieira et al., 2010), contraction level (**?**), and duration of movement and fatigue (Tucker et al., 2009; Staudenmann et al., 2014). An example of this kind of behavior is presented in Figure 2, where different spatial activation patterns of m. biceps brachii can be observed for contractions at different effort levels. In

addition, activation of individual motor units, i.e. individual motor neuron spike train, can be extracted from the HD-EMG recordings using Blind Source Separation methods (Holobar et al., 2010), **Multichannel Blind Source Separation Using Convolution Kernel Compensation**, which can be a valuable information in force estimation because motor unit recruitment and firing frequency depend primarily on force level **Merletti book**. Several authors have used this approach instead of the traditional one based on intramuscular (invasive) EMG. One of the obvious advantages of this method is that is safe and not painful, although it has not been implemented in clinical practice yet. Using this technique, authors in (Holobar et al., 2010) were able to extract 6 to 7 motor units starting from contractions at 5% MVC and up to 20% MVC with associated discharge rates between 10 pps and 12 pps. However, one of the current limitations is that the intensity of isometric contraction must remain constant during the measurement. Similar algorithms can also be used to separate EMG activity of adjacent muscles **Blind separation of linear instantaneous mixtures of nonstationary surface myoelectric signals**, (**?**). This method can be a powerful tool in task identification **Performance comparison of ICA algorithms for Isometric Hand gesture identification using Surface EMG**, because it could minimize crosstalk effect from nearby muscles. Consequently, extracted features would characterize only the target muscles. However, HD-EMG can be corrupted by low quality channels, which are a common issue in measurements due to well-known artifacts, such as: electrode displacement, bad electrical contact between skin and the electrode, movement of cables, electromagnetic interference, etc. (**?**). Affected channels differentiate themselves in amplitude and spectral content, which makes them outliers that compromise classification. To cope with this problem, authors in (Rojas-Martínez et al., 2012) developed an expert system for detection, removal and interpolation of HD-EMG channels corrupted by artifacts.

1.5 Task identification

The central nervous system (CNS) is responsible for processing information received from all parts of the body. The two main organs of the CNS are the brain and the spinal cord and are entirely composed of two kinds of specialized cells: neurons and glia. The brain is the most complex part of the human body and exerts a centralized control over the other organs.

Neurons, the basic working units of the brain, are designed to transmit information within the brain to other nerve cells and to communicate with muscles and gland cells. The complex architecture of the brain is built on the extensive number of interconnected neurons sharing information through specialized connections called synapses. This connection allows neurons to communicate through an electrical or chemical signals, producing ionic currents that generate electric and magnetic fields.

The CNS is organized in multiple levels, from simple connections between cells to coordinated cell populations, building a complex architecture of interconnected brain regions. The neural processes at this last level are produced by the dynamic coordination of smaller elements. In the cerebral cortex, all this brain activity is summed and its electric and magnetic fields can be measured on the scalp surface.

Pattern recognition is an alternative to conventional control algorithms. The prerequisite of using pattern recognition for task identification is the presence of a pattern that can be extracted from the EMG signal. Major advancement over conventional conventional switching myocontrol is the possibility of.

Pattern recognition approach doesn't support proportional and simultaneous control for multiple motor tasks. Therefore, tasks need to be performed sequentially. This type of control prevents the user from achieving a fluid movement, but also demands planning of movement execution. Although pattern recognition improves the possibility, it has serious limitations.

This implies sequential control which prevents the subject from doing fluent, e.g. Davidge et al. designed a system where movements that combine DoFs are labeled as unique classes in LDA problem, whereas Young et al. (Young et al., 2013) propose system of parallel LDA classifiers that use conditional probabilities to separate between combination of tasks.

Proportional review (Fougner et al., 2012) Force can be estimated based on the EMG : (Staudenmann et al., 2010)

In pattern recognition, there is still a large gap between industry and practice (Jiang et al., 2012).

On the other hand, one of the disadvantages of pattern recognition is the fact that in spite of the

high accuracy, an error could lead to the completely unwanted task. Also, although identification rate is usually very high during the stationary task, errors often occur during transition between tasks. This problems can be partially prevented by employing the e.g. majority voting principle (Englehart and Hudgins, 2003) (300ms, LDA), or decision-based velocity ramp that attenuates the velocity of a movement after the change of a task (Simon et al., 2011).

Challenges in pattern recognition are electrode shift (Hargrove et al., 2008; Young et al., 2011), change in arm posture (Fougner et al., 2011), slow time dependent changes (Farina et al., 2014) such as fatigue (Tkach et al., 2010), and change in electrode-skin impedance (Clancy et al., 2002).

Future works: dynamic system, hybrid system

1.5.1 Pattern recognition

Pattern recognition is a classification technique and the principle by which it is performed is learned independently from the data, i.e., training set. There are two main types of pattern recognition: supervised and unsupervised. Supervised pattern recognition implies that the classes of the training set are known and are used to obtain the model. New inputs are identified as one of the predetermined classes. On the other hand, unsupervised pattern recognition is used when no labels are available and samples are assigned to unknown classes. This technique is more appropriate for the clustering problem because the classes are determined automatically by the system, whereas supervised approach is more appropriate for the classification because classes are defined by the system designer, and, therefore, it is usually used in task identification based on EMG.

In statistical pattern recognition, each sample is composed of m measures that form the pattern, i.e., features $(x_0, x_1, \ldots, x_{m-1})$. The objective of the algorithm is to obtain a decision rule, i.e., the decision boundary which separates well samples of different classes. There are many *state-of-the-art* classifiers that use various principles to construct these boundaries. However, many researchers agree that the fidelity of the classification in EMG applications depends mostly on selection of features. In other words, with appropriate selection of features, all classifiers will give similar classification result. A short introduction is provided on the two methods used in

the thesis: Linear Discriminant Analysis and Support Vector Machine.

Linear Discriminant Analysis

All models are wrong; some models are useful.

George E. P. Box

Linear Discriminant Analysis is a computationally simple and efficient classifier with linear decision boundary and it is based on the Bayesian equation. In a classical problem with n samples in training set, which consist of m features, the dataset of available samples is a matrix of dimension $[n \times m]$, whereas the label that describes the belonging of each sample to one of the classes is y, where $y \in (0, 1, 2, ..., K-1)$.

According to Bayesian equation, the probability that a sample $\mathbf{x}_0$ belongs to a class k is equivalent to the:

$$P(y = k \mid \mathbf{x} = \mathbf{x}_0) = \frac{P(\mathbf{x} = \mathbf{x}_0 \mid y = k)\ P(y = k)}{P(\mathbf{x} = \mathbf{x}_0)} \tag{1.2}$$

, where k represents the class. Term $P(\mathbf{x} = \mathbf{x}_0 \mid y = k)$ is called the *class-conditional* probability and describes the probability that the sample with exact features $\mathbf{x}_0$ is encountered within the group of samples belonging to the class k. Term $P(y = k)$ is called the *a priori* probability and describes the probability that the sample belonging to the class k is found within the group of all samples, regardless of the features. Finally, the term $P(\mathbf{x} = \mathbf{x}_0)$ is called the *marginal* probability and describes the probability of finding the sample with exact set of features in the dataset, regardless of the class. Marginal probability can be written as a sum of class-conditional probabilities multiplied by the a priori probabilities for each class:

$$\begin{aligned} P(\mathbf{x} = \mathbf{x}_0) = P(\mathbf{x} = \mathbf{x}_0 \mid y = 1)\ P(y = 1) + \\ P(\mathbf{x} = \mathbf{x}_0 \mid y = 2)\ P(y = 2) + \cdots + \\ P(\mathbf{x} = \mathbf{x}_0 \mid y = K)\ P(y = K) \end{aligned} \tag{1.3}$$

Following the Bayesian theory, the hypothesis, i.e., the predicted class of a sample $\mathbf{x}_0$ is chosen

as the class which has the highest probability $P(y = k \mid \mathbf{x} = \mathbf{x}_0)$:

$$h(\mathbf{x}_0) = \underset{k}{\operatorname{argmax}}\, P(y = k \mid \mathbf{x} = \mathbf{x}_0) \tag{1.4}$$

Statistically speaking, this is the best possible classifier. The problem arises in the implementation. The exact probability density functions are unknown and have to be estimated from the available data, which is the source of error. Estimated version of the stated probabilities will be marked with a different symbols to stress out the fact they are just an estimates:

$$p_k(\mathbf{x}) \coloneqq P(y = k \mid \mathbf{x}) \tag{1.5}$$

$$g_k(\mathbf{x}) \coloneqq P(\mathbf{x} \mid y = k) \tag{1.6}$$

$$\pi_k \coloneqq P(y = k) \tag{1.7}$$

Linear Discriminant Analysis estimates marginal probability term (π_k) as a ratio of number of samples belonging to class k and the total number of samples, whereas the class-conditional probability term in the Bayesian equation is estimated as a multivariate Gaussian function:

$$g_k(\mathbf{x}) = \frac{1}{(2\pi)^{m/2}\,|\Sigma_k|^{1/2}}\; e^{-1/2(\mathbf{x}-\mu_k)^T\Sigma_k^{-1}(\mathbf{x}-\mu_k)} \tag{1.8}$$

, where m is the dimensionality of the feature space, i.e., number of features representing each sample. Function g_k is estimated class-conditional probability of class k, and μ_k and Σ_k are the mean and co-variance matrix for class k, respectively, and they are estimated from the available data as:

$$\mu_k = \frac{1}{n_k}\sum_i \mathbf{x}_i \Bigg|_{\forall \mathbf{x} \in k} \tag{1.9}$$

$$\Sigma_k = \frac{1}{n_k - K}\sum_i \Big(\mathbf{x}_i - \mu_k\Big)\Big(\mathbf{x}_i - \mu_k\Big)^T \Bigg|_{\forall \mathbf{x} \in k} \tag{1.10}$$

, where n_k represents the number of samples belonging to a class k. To simplify the model, LDA

assumes that the co-variance matrices Σ_k are the same for all classes:

$$\Sigma_0 = \Sigma_1 = \cdots = \Sigma_{K-1} = \Sigma \tag{1.11}$$

and they are usually calculated using the weighted average:

$$\Sigma = \frac{\sum_{k=1}^{K} n_k \Sigma_k}{\sum_{k=1}^{K} n_k} \tag{1.12}$$

The consequence of this assumption is the linearity of the decision boundary. Without this assumption the same calculus would lead to quadratic discriminant analysis, which has non-linear boundary.

In a two class example ($y \in \{0, 1\}$), all samples on the decision boundary will have the same probability of belonging to class 0 or 1:

$$D.B. = \Big\{ \mathbf{x} \;\Big|\; P\big(y = 0 \,\big|\, \mathbf{x} = \mathbf{x}_0\big) = P\big(y = 1 \,\big|\, \mathbf{x} = \mathbf{x}_0\big) \Big\} \tag{1.13}$$

Following this idea, the decision boundary can be estimated by solving the equation:

$$\frac{g_0(\mathbf{x})\,\pi_0}{\cancel{\sum_{k=1}^{K} g_k\,\pi_k}} = \frac{g_1(\mathbf{x})\,\pi_1}{\cancel{\sum_{k=1}^{K} g_k\,\pi_k}} \tag{1.14}$$

$$\frac{1}{(2\pi)^{m/2}\,|\Sigma_0|^{1/2}}\; e^{-1/2(\mathbf{x}-\mu_0)^T \Sigma_0^{-1} (\mathbf{x}-\mu_0)}\;\; \pi_0 = \frac{1}{(2\pi)^{m/2}\,|\Sigma_1|^{1/2}}\; e^{-1/2(\mathbf{x}-\mu_1)^T \Sigma_1^{-1} (\mathbf{x}-\mu_1)}\;\; \pi_1 \tag{1.15}$$

If making the assumption on the equal co-variance matrices for both classes ($\Sigma_0 = \Sigma_1 = \Sigma$), and taking the logarithm, the equation takes the form:

$$-\frac{1}{2}\Big(\mathbf{x} - \mu_0\Big)^T \Sigma^{-1} \Big(\mathbf{x} - \mu_0\Big) + \log\Big(\pi_0\Big) = -\frac{1}{2}\Big(\mathbf{x} - \mu_1\Big)^T \Sigma^{-1} \Big(\mathbf{x} - \mu_1\Big) + \log\Big(\pi_1\Big) \tag{1.16}$$

, which can be written in the form of the linear function $x^T\beta + \alpha = 0$ as:

$$\mathbf{x}^T\Big(\Sigma^{-1}\mu_0 - \Sigma^{-1}\mu_1\Big) + \frac{1}{2}\Big(\mu_1^T\Sigma^{-1}\mu_1 - \mu_0^T\Sigma^{-1}\mu_0\Big) + \log\Big(\frac{\pi_0}{\pi_1}\Big) = 0 \tag{1.17}$$

This equation represents the decision boundary between two classes, i.e., all samples lying on this line will have equal probability of belonging to class 0 and class 1. It should be noted that the slope of the line depends only on the class means and co-variance matrix, whereas a priori probabilities (which are the result of number of samples belonging to class 0 or 1) have effect only on the y-intercept term, i.e., the offset of the function. This is an interesting point that demands caution. If groups are unbalanced, that is, number of samples of one group is higher than in the other group, y-intercept of the decision boundary will be affected and the classifier will be biased by this disproportion. If groups are unbalanced because of the incomplete or missing data, whereas in reality they are balanced, this can have a negative effect.

When considering multiclass classification problem, probability of a sample belonging to each class is firstly estimated by the equation:

$$p_k = -\frac{1}{2}\log|\Sigma| - \frac{1}{2}\Big(\mathbf{x} - \mu_k\Big)^T\Sigma^{-1}\Big(\mathbf{x} - \mu_k\Big) + \log\Big(\pi_k\Big) \tag{1.18}$$

and then the class is estimated as the one with the highest probability as:

$$h(\mathbf{x}) = \underset{k}{\operatorname{argmax}}\, p_k(\mathbf{x}) \tag{1.19}$$

Support Vector Machine

> *Try to solve the problem directly and never solve a more general problem as an intermediate step.*
>
> Vladimir Vapnik

Support vector machine is nowadays known as a very powerful classifier with a lot of different applications. The big advantage over LDA is the fact that it is a *non-parametric* classifier. The model is not obtained using assumptions of the form of the class density function and estimation

of it's parameters, which is inevitably erroneous. Instead, SVM forms the decision boundary using the samples (not their density estimates) by maximizing the distance between samples and the boundary. This was the idea Vladimir Vapnik, the inventor of this method stood for. It is better to try to solve the problem directly and simply, without many intermediate steps that can be complicated and inaccurate.

In pattern recognition, the decision rule (h) is usually obtained by multiplying the sample ($\mathbf{x}$) by predefined weights (Θ):

$$\Theta^T \mathbf{x} + \Theta_0 \tag{1.20}$$

, where Θ_0 is a constant. If samples $\mathbf{x}_0$ and $\mathbf{x}_1$ lay on the decision boundary, following statements are true:

$$\Theta^T \mathbf{x}_0 + \Theta_0 = \Theta^T \mathbf{x}_1 + \Theta_0 \tag{1.21}$$

$$\Theta^T (\mathbf{x}_0 - \mathbf{x}_1) = 0 \tag{1.22}$$

This result implies that Θ is perpendicular to the boundary:

$$\Theta \perp (\mathbf{x}_0 - \mathbf{x}_1) \tag{1.23}$$

The goal of the SVM is to find the decision boundary between two classes so that the distance between the samples and the decision boundary, i.e., the margin is maximized. The distance (d) from a sample to the decision boundary can be defined as the distance between the sample $\mathbf{x}$ and any point lying on the boundary, $\mathbf{x}_0$, projected onto the vector Θ.

$$d = \frac{\Theta^T \big(\mathbf{x} - \mathbf{x}_0\big)}{\big|\Theta\big|} \tag{1.24}$$

Term $|\Theta|$ is introduced to normalize the vector Θ. Without the normalization the distance would depend on the norm of Θ.

Since $\mathbf{x}_0$ is on the decision boundary, the expression $\Theta^T \mathbf{x}_0 + \Theta_0 = 0$ is valid, and, therefore, the

expression for the distance can be written as:

$$d = \frac{\Theta^T \mathbf{x} + \Theta_0}{|\Theta|} \tag{1.25}$$

Margin (M) can be defined as the distance from the boundary to the closest sample:

$$M = \min_i d_i \tag{1.26}$$

Depending on which side of the boundary the sample is located, the distance can be positive or negative. In order to keep it strictly positive, term y is introduced, where $y \in \{-1, 1\}$:

$$M = \min_i \left\{ y_i d_i \right\} \tag{1.27}$$

$$M = \min_i \left\{ \frac{y_i \left(\Theta^T \mathbf{x}_i + \Theta_0 \right)}{|\Theta|} \right\} \tag{1.28}$$

The objective is to maximize the margin M. Since Θ can be rescaled, a certain Θ exists so that $y_i \left(\Theta^T \mathbf{x}_i + \Theta_0 \right) = 1$, which implies

$$\exists \Theta,\ y_i \left(\Theta^T \mathbf{x}_i + \Theta_0 \right) = 1 \quad \Rightarrow \quad M = \min_i \left\{ \frac{1}{|\Theta|} \right\} \tag{1.29}$$

Therefore, to maximize the margin, a separating hyperplane should be found such that a norm of vector orthogonal to the hyperplane (Θ) is minimal.

For every point not on the boundary the following term is valid:

$$y_i \left(\Theta^T \mathbf{x}_i + \Theta_0 \right) > 0 \tag{1.30}$$

Value C can be selected such that:

$$y_i \left(\Theta^T \mathbf{x}_i + \Theta_0 \right) > C \tag{1.31}$$

$$y_i \left(\frac{\Theta^T \mathbf{x}_i}{C} + \frac{\Theta_0}{C} \right) > 1 \tag{1.32}$$

Since Θ and Θ_0 can be rescaled, it can be written:

$$\Theta := \frac{\Theta}{C}, \quad \Theta_0 := \frac{\Theta_0}{C} \tag{1.33}$$

, and, therefore:

$$y_i \left(\Theta^T \mathbf{x}_i + \Theta_0 \right) > 1 \tag{1.34}$$

Finally the optimization problem states:

$$\min \frac{1}{2} |\Theta|^2, \quad s.t. \; y_i \left(\Theta^T \mathbf{x}_i + \Theta_0 \right) > 1. \tag{1.35}$$

L_2 norm is preferred because it has continuous derivative, whereas constant $1/2$ is introduced for the mathematical convenience. The optimization is solved using Lagrangian method as:

$$L(\Theta, \Theta_0, \alpha_i) = \frac{1}{2} |\Theta|^2 - \sum_{i=1}^{n} \alpha_i \left[y_i \left(\Theta^T \mathbf{x}_i + \Theta_0 \right) - 1 \right] \tag{1.36}$$

$$\frac{\partial L}{\partial \Theta} = \Theta - \sum_{i=1}^{n} \alpha_i y_i \mathbf{x}_i = 0 \quad \Rightarrow \quad \Theta = \sum_{i=1}^{n} \alpha_i y_i \mathbf{x}_i \tag{1.37}$$

$$\frac{\partial L}{\partial \Theta_0} = \sum_{i=1}^{n} \alpha_i y_i = 0 \tag{1.38}$$

By rewriting the problem in 1.36 in terms of dual variable α, the following expression can be obtained:

$$L(\alpha) = \sum_i \alpha_i - \frac{1}{2} \sum_j \sum_i \alpha_j \alpha_i y_j y_i \mathbf{x}_i^T \mathbf{x}_j \tag{1.39}$$

Since this function depends only on dual variable α, the solution can be obtained by maximiza-

tion:

$$\max L(\alpha) \quad s.t. \quad \begin{cases} \alpha_i \geq 0 \\ \sum_i \alpha_i y_i = 0 \end{cases} \tag{1.40}$$

In this optimization problem, the objective has the form of quadratic function, whereas constraints are linear. This problem is typically solved using quadratic programming. Since it is a convex problem, the solution will always be global maximum. Once the dual variable α is found, the primal variable Θ can be calculated using the equation 1.37.

In the optimization, Karush-Kuhn-Tucker conditions need to be satisfied (Boyd and Vandenberghe, 2004). One of this condition is *complementary slackness*, stating that in the optimal point (the solution of the problem), the product of dual variable and the constraint must be zero:

$$\alpha_i \left[y_i \left(\Theta^T \mathbf{x}_i + \Theta_0 \right) - 1 \right] = 0 \tag{1.41}$$

This condition explains well the principle of SVM. Since the dual variable must be greater or equal to zero ($\alpha \geq 0$), there are two possibilities:

1. If α is greater than zero, $\left[y_i \left(\Theta^T \mathbf{x}_i + \Theta_0 \right) - 1 \right]$ must equal one:

$$\alpha_i > 0 \quad \Rightarrow \quad y_i \left(\Theta^T \mathbf{x}_i + \Theta_0 \right) = 1 \tag{1.42}$$

2. If $\left[y_i \left(\Theta^T \mathbf{x}_i + \Theta_0 \right) - 1 \right]$ is greater than zero, α must be zero:

$$y_i \left(\Theta^T \mathbf{x}_i + \Theta_0 \right) > 1 \quad \Rightarrow \quad \alpha = 0 \tag{1.43}$$

Since for all samples lying on the margin, the statement

$$y_i \left(\Theta^T \mathbf{x}_i + \Theta_0 \right) = 1 \tag{1.44}$$

holds, α will be greater than zero only for the samples lying on the decision hyperplane, whereas for the samples further away from the hyperplane, α will be zero. Given the fact that Θ depends on linear combination of samples weighted by α (eq. 1.37), only the samples lying

on the boundary will have effect in the calculation of Θ (where $\alpha > 0$), and they are called *support vectors*. The inconveniency of this approach is the fact that the data need to be linearly separable, i.e., there should not be any data on the other side of the margin, which is rarely the case in practice. For this reason it is called the *hard margin SVM*. Margin has distance one from the boundary and all points have to be distanced more or equal (constraint in eq. 1.34). To relax this constrain, variable β_i is introduced for every sample $\mathbf{x}_i$, such that $\beta_i \geq 0$:s

$$y_i \left(\Theta^T \mathbf{x}_i + \Theta_0\right) \geq 1 - \beta_i \tag{1.45}$$

For points lying on the other side of the margin, β will be positive, whereas for the points on the margin or on the correct side of it, it will be zero. This is the ground assumption for *soft margin SVM*. The new optimization problem states:

$$\max \frac{1}{2}|\Theta|^2 + \gamma \sum_{i=1}^{n} \beta_i \quad s.t. \quad \begin{cases} y_i \left(\Theta^T \mathbf{x}_i + \Theta_0\right) \geq 1 - \beta_i \\ \beta_i \geq 0 \end{cases} \tag{1.46}$$

The term $\gamma \sum_{i=1}^{n} \beta_i$ is introduced to minimize this effect, whereas γ is the constant of penalization. The procedure of solving the problem is the same as in hard margin SVM, using the Lagrangian method:

$$L(\Theta, \Theta_0, \beta_i, \alpha_i, \lambda_i) = \frac{1}{2}|\Theta|^2 + \gamma \sum_{i=1}^{n} \beta_i - \sum_{i=1}^{n} \alpha_i \left[y_i \left(\Theta^T \mathbf{x}_i + \Theta_0\right) - 1 + \gamma\beta_i\right] - \sum_{i=1}^{n} \lambda_i \beta_i \tag{1.47}$$

$$\frac{\partial L}{\partial \Theta} = \Theta - \sum_{i=1}^{n} \alpha_i y_i \mathbf{x}_i = 0 \quad \Rightarrow \quad \Theta = \sum_{i=1}^{n} \alpha_i y_i \mathbf{x}_i \tag{1.48}$$

$$\frac{\partial L}{\partial \Theta_0} = \sum_{i=1}^{n} \alpha_i y_i = 0 \tag{1.49}$$

$$\frac{\partial L}{\partial \beta_i} = \gamma - \alpha_i - \lambda_i = 0 \tag{1.50}$$

By rewriting the optimization problem in terms of dual variable α, the same term can be obtained

as in eq. 1.39:

$$L(\alpha) = \sum_i \alpha_i - \frac{1}{2} \sum_j \sum_i \alpha_j \alpha_i y_j y_i \mathbf{x}_i^T \mathbf{x}_j \tag{1.51}$$

, and the new optimization problem states:

$$\max L(\alpha) \quad s.t. \quad \begin{cases} \alpha_i \geq 0 \\ \lambda_i \geq 0 \end{cases} \tag{1.52}$$

However, since objective function $L(\alpha)$ does not depend on dual variable λ_i, the substituation can be made following the expression in eq. 1.50 and the new optimization problem states:

$$\max L(\alpha) \quad s.t. \ 0 \leq \alpha_i \leq \gamma. \tag{1.53}$$

This is the only diference between hard margin SVM and soft margin SVM.

It is important to state that the optimization problem does not depend on $\mathbf{x}$, but on $\mathbf{x}^T\mathbf{x}$. This allows the use of *kernel trick* and implicitly enables nonlinear transform of the feature space at little additional cost. Usually, non-linear decision boundary can be achieved by nonlinear transform of features:

$$\mathbf{x} \rightarrow \Phi(\mathbf{x}) \tag{1.54}$$

However, this operation is computationally expensive. The solution can be achieved using kernel functions. Kernel is a function $K(x, y)$ for which:

$$K(\mathbf{x}, \mathbf{y}) = \Phi(\mathbf{x})^T \Phi(\mathbf{y}) \tag{1.55}$$

Since in the equation 1.38 $\mathbf{x}$ does not appear by itself, but in a form of dot product $\mathbf{x}^T\mathbf{x}$, non-linear transform can be used in a form of kernel trick:

$$L(\alpha) = \sum_i \alpha_i - \frac{1}{2} \sum_j \sum_i \alpha_j \alpha_i y_j y_i K(\mathbf{x}_i, \mathbf{x}_j) \tag{1.56}$$

Most often used kernel is a radial basis kernel ($K_{RBF}(\mathbf{x}_i, \mathbf{x}_j)$):

$$K_{RBF}(\mathbf{x}_i, \mathbf{x}_j) = e^{\frac{-\|\mathbf{x}_i - \mathbf{x}_j\|^2}{2\sigma^2}} \tag{1.57}$$

Although SVM is conceptually designed as a two-class classifier, techniques for multiclass classification also exist, e.g. *one-versus-one* or *one-versus-all*.

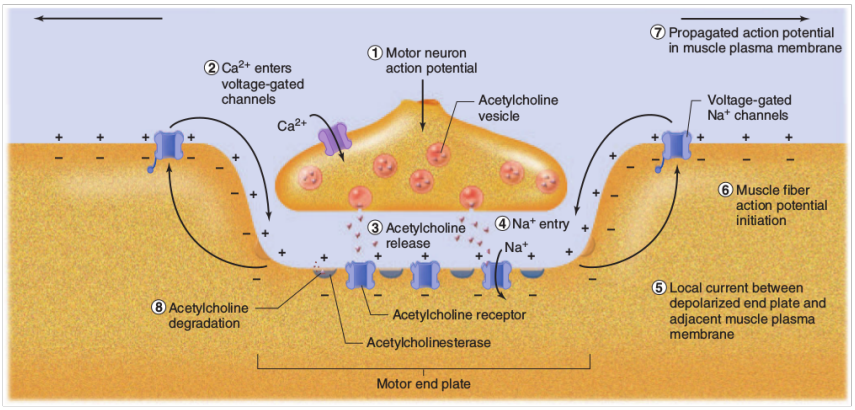

Figure 1.2: Ilustration of generation of action potential. Adopted from citepWidmaier

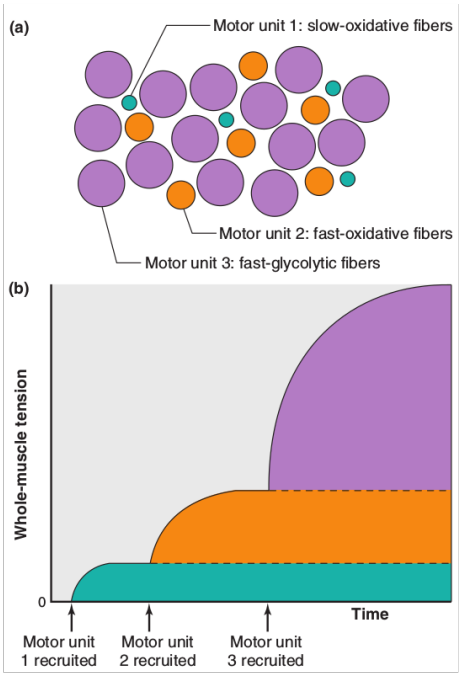

Figure 1.3: Figure illustrates **a)** diagram of different muscle fibers in muscle cross section, and **b)** muscle tension produced by recruitment of different types of muscle fiber. It can be noted that type S fibers are activated first and generate low force level, whereas type FF fibers are activated last and generate high forces . Adopted from Widmaier

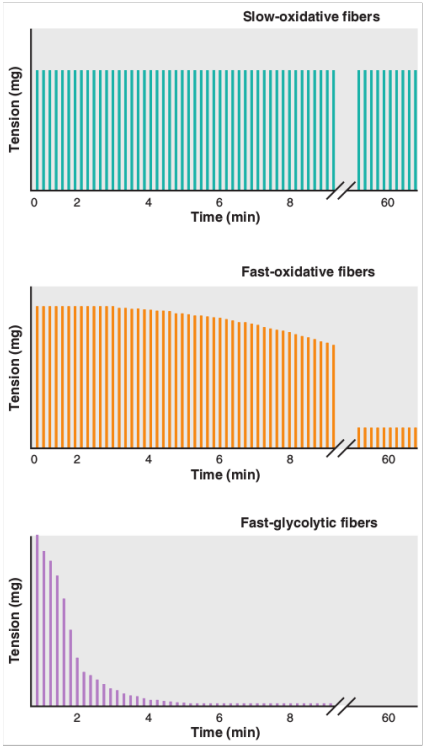

Figure 1.4: Figure illustrates the time during which specific muscle fibers can remain tension. Adopted from Widmaier

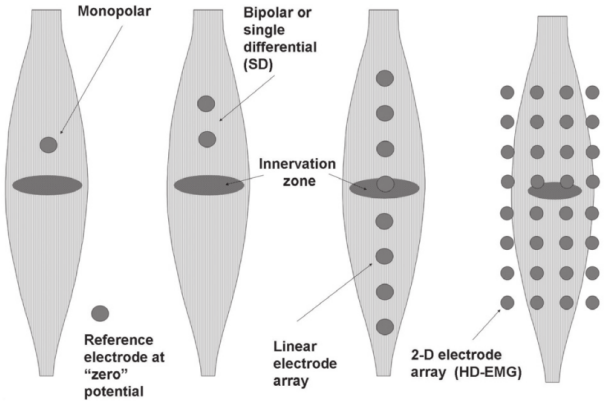

Figure 1.5: Four types of recording surface EMG signal: monopolar, bipolar, linear electrode array, HD-EMG. Figure was modified from (Merletti et al., 2010) Traditional monopolar detection with respect to a remote reference taken as zero (reference) potential. b) Bipolar (or single differential, SD) detection (or mon- tage) along the fiber direction. c) Linear (one dimensional, 1-D) array of electrodes along the fiber direction. Spatial filters (such as double or N-differential) can be obtained by properly weighting and adding the signals from nearby electrodes. d) 2-dimensional (2-D) array of electrodes providing an image of potential distribution. Spatial filters (such as double or N-differential in the column or row direction, Laplacian, inverse binomial, etc.) may be applied to the signals. Image processing procedures may be applied to the "image" to interpolate or virtually rotate the image to align it with the fiber direction or to detect edges or areas of high or low activity or gradient. are

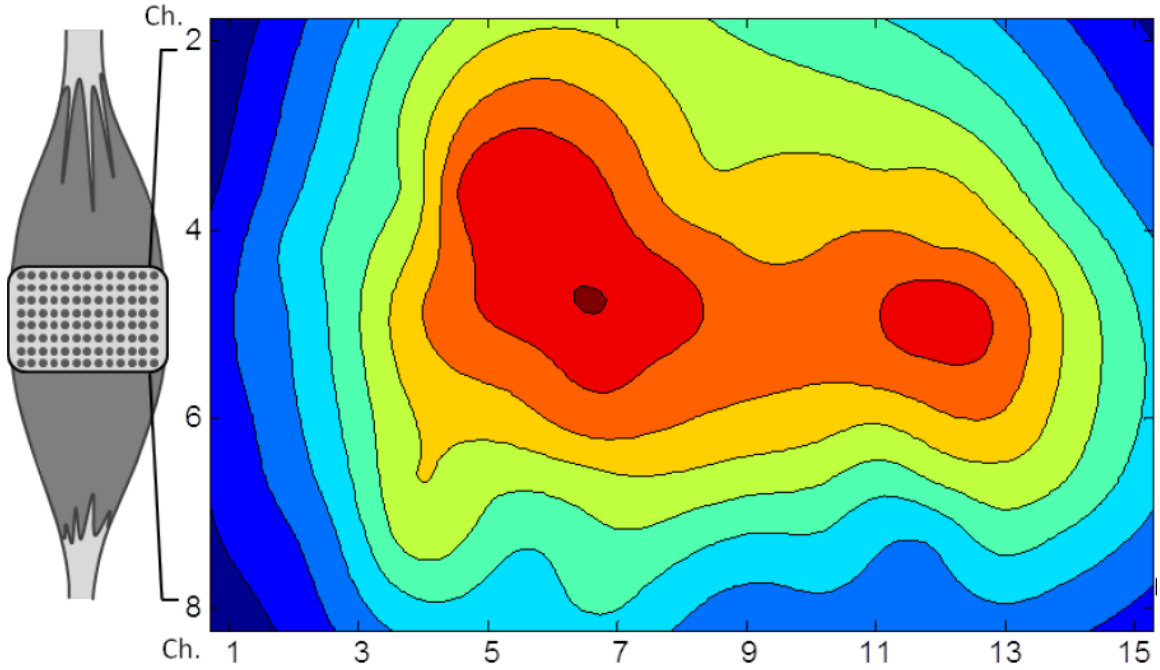

Figure 1.6: The figure represents the HD-EMG activation map recorded on the biceps brachii muscle during flexion. Distinct activation of the two heads can be noticed in the map. Modified from Monica

Bibliography

MATLAB and Statistics and Machine Learning Toolbox Release 2015a.

Ameri, A., Englehart, K. B., and Parker, P. a. A comparison between force and position control strategies in myoelectric prostheses. *Proceedings of the Annual International Conference of the IEEE Engineering in Medicine and Biology Society, EMBS*, pages 1342–1345, 2012.

Boschmann, A. and Platzner, M. Reducing the Limb Position Effect in Pattern Recognition Based Myoelectric Control using a High Density Electrode Array. *2013 ISSNIP Biosignals and Biorobotics Conference (BRC)*, pages 1–5, 2013.

Boyd, S. and Vandenberghe, L. *Convex optimization*. Cambridge University Press, 2004.

Cacoullos, T. Estimation of a multivariate density. *Annals of the Institute of Statistical Mathematics*, 18(1):179–189, 1966.

Celadon, N., Došen, S., Binder, I., Ariano, P., and Farina, D. Proportional estimation of finger movements from high-density surface electromyography. *Journal of NeuroEngineering and Rehabilitation*, 2016.

Clancy, E., Morin, E. L., and Merletti, R. Sampling, noise-reduction and amplitude estimation issues in surface electromyography. *Journal of Electromyography and Kinesiology*, 12(1):1–16, 2002.

Comaniciu, D. and Meer, P. Mean shift: a robust approach toward feature space analysis. *IEEE Transactions on Pattern Analysis and Machine Intelligence*, 24(5):603–619, 2002.

De Luca, C. J. Myoelectrical manifestations of localized muscular fatigue in humans. *Critical Reviews in Biomedical Engineering*, 11(4):251–79, jan 1984.

De Luca, C. J. The use of surface electromyography in biomechanics. *Journal of Applied Biomechanics*, 13(2):135–163, 1997.

Dipietro, L., Ferraro, M., Palazzolo, J. J., Krebs, H. I., Volpe, B. T., and Hogan, N. Customized interactive robotic treatment for stroke: EMG-triggered therapy. *IEEE Transactions on Neural Systems and Rehabilitation Engineering*, 13(3):325–334, 2005.

Du, Y., Jin, W., Wei, W., Hu, Y., and Geng, W. Surface EMG-Based Inter-Session Gesture Recognition Enhanced by Deep Domain Adaptation. *Sensors*, 17(3):458, 2017.

Duchateau, J. and Enoka, R. M. Human motor unit recordings: Origins and insight into the integrated motor system. *Brain Research*, 1409:42–61, 2011.

Englehart, K. and Hudgins, B. A robust, real-time control scheme for multifunction myoelectric control. *IEEE Transactions on Biomedical Engineering*, 50(7):848–854, 2003.

Farina, D., Colombo, R., Merletti, R., and Olsen, H. B. Evaluation of intra-muscular EMG signal decomposition algorithms. *Journal of Electromyography and Kinesiology*, 11(3):175–187, 2001.

Farina, D., Holobar, A., Merletti, R., and Enoka, R. M. Decoding the neural drive to muscles from the surface electromyogram. *Clinical Neurophysiology*, 121(10):1616–1623, 2010.

Farina, D., Jiang, N., Rehbaum, H., Holobar, A., Graimann, B., Dietl, H., and Aszmann, O. C. The extraction of neural information from the surface EMG for the control of upper-limb prostheses: emerging avenues and challenges. *IEEE Transactions on Neural Systems and Rehabilitation Engineering*, 22(4):797–809, 2014.

Fougner, A., Scheme, E., Chan, A. D. C., Englehart, K., and Stavdahl, Ø. Resolving the Limb Position Effect in Myoelectric Pattern Recognition. *IEEE Transactions on Neural Systems and Rehabilitation Engineering*, 19(6):644–651, 2011.

Fougner, A., Stavdahl, O., Kyberd, P. J., Losier, Y. G., and Parker, P. a. Control of upper limb prostheses: Terminology and proportional myoelectric control - A review. *IEEE Transactions on Neural Systems and Rehabilitation Engineering*, 20(5):663–677, 2012.

Freund, H. J., Büdingen, H. J., and Dietz, V. Activity of Single Motor Units from Human Forearm Muscles during Voluntary Isometric Contractions. *Journal of Neurophysiology*, 38 (4):933–46, jul 1975.

Fukunaga, K. and Hostetler, L. The estimation of the gradient of a density function, with applications in pattern recognition. *IEEE Transactions on Information Theory*, 21(1):32–40, 1975.

Geng, W., Du, Y., Jin, W., Wei, W., Hu, Y., and Li, J. Gesture recognition by instantaneous surface EMG images. *Scientific Reports*, 6(1):36571, 2016.

Geng, Y., Zhang, X., Zhang, Y.-T., and Li, G. A novel channel selection method for multiple motion classification using high-density electromyography. *Biomedical Engineering Online*, 13:102, 2014.

Greenhouse, S. W. and Geisser, S. On methods in the analysis of profile data. *Psychometrika*, 24(2):95–112, 1959.

Grouven, U., Bergel, F., and Schultz, A. Implementation of linear and quadratic discriminant analysis incorporating costs of misclassification. *Computer Methods and Programs in Biomedicine*, 49(1):55–60, jan 1996.

Hahne, J. M., Graimann, B., and Muller, K. R. Spatial filtering for robust myoelectric control. *IEEE Transactions on Biomedical Engineering*, 59(5):1436–1443, 2012.

Hahne, J. M., Dähne, S., Hwang, H. J., Müller, K. R., and Parra, L. C. Concurrent Adaptation of Human and Machine Improves Simultaneous and Proportional Myoelectric Control. *IEEE Transactions on Neural Systems and Rehabilitation Engineering*, 23(4):618–627, 2015.

Hakonen, M., Piitulainen, H., and Visala, A. Current state of digital signal processing in myoelectric interfaces and related applications. *Biomedical Signal Processing and Control*, 18: 334–359, 2015.

Hargrove, L., Englehart, K., and Hudgins, B. A training strategy to reduce classification degradation due to electrode displacements in pattern recognition based myoelectric control. *Biomedical Signal Processing and Control*, 3(2):175–180, 2008.

Hargrove, L., Li, G., Englehart, K., and Hudgins, B. Principal Components Analysis Preprocessing for Improved Classification Accuracies in Pattern-Recognition-Based Myoelectric Control. *IEEE Transactions on Biomedical Engineering*, 56(5):1407–1414, 2009.

Hargrove, L. J., Englehart, K., and Hudgins, B. A comparison of surface and intramuscular myoelectric signal classification. *IEEE Transactions on Biomedical Engineering*, 54(5):847–853, 2007.

He, J., Zhang, D., Sheng, X., Li, S., and Zhu, X. Invariant surface EMG feature against varying contraction level for myoelectric control based on muscle coordination. *IEEE Journal of Biomedical and Health Informatics*, 19(3):874–882, 2015.

Henneberg, K. Principles of Electromyography. In Bronzino, J., editor, *The Biomedical Engineering Handbook*. CRC Press, Boca Raton, second edition, 1999.

Henneman, E., Somjen, G., and Carpenter, D. O. Functional Significance of Cell Size in Spinal Motoneurons. *Journal of Neurophysiology*, 28(3), 1965.

Hennig, C., Meila, M., Murtagh, F., and Rocci, R. *Handbook of Cluster Analysis*. CRC Press, 2015.

Hermens, H. and Freriks, B. *SENIAM 9: European Recommendations for Surface ElectroMyoGraphy, results of the SENIAM project (CD)*. Roessingh Research and Development, 1999.

Hogan, N., Krebs, H. I., Rohrer, B., Palazzolo, J. J., Dipietro, L., Fasoli, S. E., Stein, J., Hughes, R., Frontera, W. R., Lynch, D., and Volpe, B. T. Motions or muscles? Some behavioral factors underlying robotic assistance of motor recovery. *Journal of Rehabilitation Research and Development*, 43(5):605–618, 2006.

Holobar, A., Minetto, M. A., Botter, A., Negro, F., and Farina, D. Experimental Analysis of Accuracy in the Identification of Motor Unit Spike Trains From High-Density Surface EMG. *IEEE Transactions on Neural Systems and Rehabilitation Engineering*, 18(3):221–229, 2010.

Holtermann, A., Roeleveld, K., and Karlsson, J. S. Inhomogeneities in muscle activation reveal motor unit recruitment. *Journal of Electromyography and Kinesiology*, 15(2):131–137, apr 2005.

Huang, H., Zhou, P., Li, G., and Kuiken, T. Spatial filtering improves EMG classification accuracy following targeted muscle reinnervation. *Annals of biomedical engineering*, 37(9): 1849–57, 2009.

Huang, Y., Englehart, K. B., Hudgins, B., and Chan, A. D. C. A Gaussian mixture model based classification scheme for myoelectric control of powered upper limb prostheses. *IEEE Transactions on Biomedical Engineering*, 52(11):1801–1811, 2005.

Jiang, N., Dosen, S., Muller, K.-R., and Farina, D. Myoelectric Control of Artificial Limbs—Is There a Need to Change Focus? [In the Spotlight]. *IEEE Signal Processing Magazine*, 29(5): 152–150, 2012.

Jordanic, M., Rojas-Martínez, M., Mañanas, M. A., and Alonso, J. F. Spatial distribution of HD-EMG improves identification of task and force in patients with incomplete spinal cord injury. *Journal of NeuroEngineering and Rehabilitation*, 13(1):41, 2016.

Jordanić, M., Rojas-Martínez, M., Mañanas, M. A., and Alonso, J. F. Prediction of isometric motor tasks and effort levels based on high-density EMG in patients with incomplete spinal cord injury. *Journal of Neural Engineering*, 13(4):046002, 2016.

Kendall, F. P., Kendall McCreary, E., and Provance, P. G. *Muscles: testing and function.* Williams & Wilkins, New York, 4 edition, 1993.

Landa, S. and Everitt, B. S. *A Handbook of Statistical Analyses using SPSS.* Chapman & Hall/CRC, Boca Raton, 2004.

Li, G., Schultz, A. E., and Kuiken, T. A. Quantifying pattern recognition- based myoelectric control of multifunctional transradial prostheses. *IEEE Transactions on Neural Systems and Rehabilitation Engineering*, 18(2):185–192, 2010.

Li, X., Samuel, O. W., Zhang, X., Wang, H., Fang, P., and Li, G. A motion-classification strategy based on sEMG-EEG signal combination for upper-limb amputees. *Journal of NeuroEngineering and Rehabilitation*, 14(1):2, 2017.

Li, Y., Chen, X., Zhang, X., and Zhou, P. Several practical issues toward implementing myoelectric pattern recognition for stroke rehabilitation. *Medical Engineering and Physics*, 36(6): 754–760, 2014.

Li, Z., Wang, B., Yang, C., Xie, Q., and Su, C. Y. Boosting-based EMG patterns classification scheme for robustness enhancement. *IEEE Journal of Biomedical and Health Informatics*, 2013.

Liddell, E. G. T. and Sherrington, C. S. Recruitment and some other Features of Reflex Inhibition. *Proceedings of the Royal Society of London B: Biological Sciences*, 97(686):488–518, 1925.

Liu, J. and Zhou, P. A novel myoelectric pattern recognition strategy for hand function restoration after incomplete cervical spinal cord injury. *IEEE Transactions on Neural Systems and Rehabilitation Engineering*, 21(1):96–103, 2013.

Liu, J., Sheng, X., Zhang, D., Jiang, N., and Zhu, X. Towards Zero Retraining for Myoelectric Control Based on Common Model Component Analysis. *IEEE Transactions on Neural Systems and Rehabilitation Engineering*, 24(4):444–454, 2016.

Loftus, G. R. and Masson, M. E. Using confidence intervals in within-subject designs. *Psychonomic bulletin & review*, 1(4):476–90, 1994.

Mañanas, M., Romero, S., Topor, Z., Bruce, E., Houtz, P., and Caminal, P. Cardiac interference in myographic signals from different respiratory muscles and levels of activity. *2001 Conference Proceedings of the 23rd Annual International Conference of the IEEE Engineering in Medicine and Biology Society*, 2:1115–1118, 2001.

Marateb, H. R., McGill, K. C., and Webster, J. G. Electromyographic (Emg) Decomposition. In *Wiley Encyclopedia of Electrical and Electronics Engineering.* John Wiley & Sons, Inc, 1999.

Marateb, H. R., Farahi, M., Rojas, M., Mañanas, M. A., Farina, D., and Rix, H. Detection of Multiple Innervation Zones from Multi-Channel Surface EMG Recordings with Low Signal-to-Noise Ratio Using Graph-Cut Segmentation. *PLOS ONE*, 11(12), 2016.

Marchal-Crespo, L. and Reinkensmeyer, D. J. Review of control strategies for robotic movement training after neurologic injury. *Journal of Neuroengineering and Rehabilitation*, 6:20, 2009.

Merletti, R. and Farina, D. *Surface Electromyography: Physiology, Engineering, and Applications*. Wiley-IEEE Press, Hoboken, New Jersey (USA), 2016.

Merletti, R. and Hermens, H. Detection and Conditioning of the surface EMG signal. In *Electromyography: Physiology, Engineering, and Noninvasive Applications*, chapter 5, pages 115–120. Wiley, New Jersey, USA, 2004.

Merletti, R. and Parker, P. *Electromyography : physiology, engineering, and noninvasive applications*. Wiley-IEEE Press, 2004.

Merletti, R., Botter, A., Troiano, A., Merlo, E., and Minetto, M. A. Technology and instrumentation for detection and conditioning of the surface electromyographic signal: State of the art. *Clinical Biomechanics*, 24(2):122–134, 2009.

Merletti, R., Aventaggiato, M., Botter, A., Holobar, A., Marateb, H., and Vieira, T. M. M. Advances in surface EMG: recent progress in detection and processing techniques. *Critical Reviews in Biomedical Engineering*, 38(4):305–45, 2010.

Mohebian, M. R., Marateb, H. R., Mansourian, M., Mañanas, M. A., and Mokarian, F. A Hybrid Computer-aided-diagnosis System for Prediction of Breast Cancer Recurrence (HPBCR) Using Optimized Ensemble Learning. *Computational and Structural Biotechnology Journal*, 15:75–85, 2017.

Mosteller, F. A k-Sample Slippage Test for an Extreme Population on JSTOR. *The Annals of Mathematical Statistics*, 19(1):58–65, 1948.

Muller-Putz, G., Leeb, R., Tangermann, M., Hohne, J. H., Kubler, A. K., Cincotti, F., Mattia, D., Rupp, R., Muller, K. R., and Millan, J. D. R. Towards Noninvasive Hybrid Brain–Computer Interfaces: Framework, Practice, Clinical Application, and Beyond. *Proceedings of the IEEE*, 103(6):926 – 943, 2015.

Nazmi, N., Abdul Rahman, M., Yamamoto, S.-I., Ahmad, S., Zamzuri, H., and Mazlan, S. A Review of Classification Techniques of EMG Signals during Isotonic and Isometric Contractions. *Sensors*, 16(8):1304, 2016.

Oskoei, M. A. and Hu, H. GA-based feature subset selection for myoelectric classification. *2006 IEEE International Conference on Robotics and Biomimetics, ROBIO 2006*, pages 1465–1470, 2006.

Oskoei, M. A. and Hu, H. Myoelectric control systems-A survey. *Biomedical Signal Processing and Control*, 2(4):275–294, 2007.

Parker, P., Englehart, K., and Hudgins, B. Myoelectric signal processing for control of powered limb prostheses. *Journal of Electromyography and Kinesiology*, 16:541–548, 2006.

Parzen, E. On Estimation of a Probability Density Function and Mode. *The Annals of Mathematical Statistics*, 33(3):1065–1076, 1962.

Pedregosa, F., Varoquaux, G., Gramfort, A., Michel, V., Thirion, B., Grisel, O., Blondel, M., Prettenhofer, P., Weiss, R., Dubourg, V., Vanderplas, J., Passos, A., Cournapeau, D., Brucher, M., Perrot, M., and Duchesnay, E. Scikit-learn: Machine Learning in Python. *Journal of Machine Learning Research*, 12:2825–2830, 2011.

Pizzigalli, L., Ahmaidi, S., and Rainoldi, A. Effects of sedentary condition and longterm physical activity on postural balance and strength responses in elderly subjects. *Sport Sciences for Health*, 10(2):135–141, 2014.

Rohm, M., Schneiders, M., Müller, C., Kreilinger, A., Kaiser, V., Müller-Putz, G. R., and Rupp, R. Hybrid brain-computer interfaces and hybrid neuroprostheses for restoration of upper limb functions in individuals with high-level spinal cord injury. *Artificial Intelligence in Medicine*, 59(2):133–142, 2013.

Rojas-Martínez, M., Mañanas, M. a., and Alonso, J. F. High-density surface EMG maps from upper-arm and forearm muscles. *Journal of Neuroengineering and Rehabilitation*, 9:85, jan 2012.

Rojas-Martínez, M., Mañanas, M. a., Alonso, J. F., and Merletti, R. Identification of isometric contractions based on High Density EMG maps. *Journal of Electromyography and Kinesiology*, 23(1):33–42, 2013.

Scheme, E. and Englehart, K. Training strategies for mitigating the effect of proportional control on classification in pattern recognition-based myoelectric control. *Journal of Prosthetics and Orthotics*, 25(2):76–83, 2013.

Searle, A. and Kirkup, L. A direct comparison of wet, dry and insulating bioelectric recording electrodes. *Physiological Measurement*, 21(2):271–83, 2000.

Sensinger, J., Lock, B., and Kuiken, T. Adaptive Pattern Recognition of Myoelectric Signals: Exploration of Conceptual Framework and Practical Algorithms. *IEEE Transactions on Neural Systems and Rehabilitation Engineering*, 17(3):270–278, 2009.

Sherrington, C. S. Remarks on some Aspects of Reflex Inhibition. *Proceedings of the Royal Society of London B: Biological Sciences*, 97(686):519–545, 1925.

Simon, A. M., Hargrove, L. J., Lock, B. a., and Kuiken, T. a. A decision-based velocity ramp for minimizing the effect of misclassifications during real-time pattern recognition control. *IEEE Transactions on Biomedical Engineering*, 58(8):2360–2368, 2011.

Squire, J. *Muscle: design, diversity, and disease*. Benjamin/Cummnigs, Menlo Park, CA, USA, 1986.

Stango, A., Negro, F., and Farina, D. Spatial Correlation of High Density EMG Signals Provides Features Robust to Electrode Number and Shift in Pattern Recognition for Myocontrol. *IEEE Transactions on Neural Systems and Rehabilitation Engineering*, 23(2):189–198, 2015.

Staudenmann, D., Roeleveld, K., Stegeman, D. F., and van Dieen, J. H. Methodological aspects of SEMG recordings for force estimation - A tutorial and review. *Journal of Electromyography and Kinesiology*, 20(3):375–387, 2010.

Staudenmann, D., van Dieën, J. H., Stegeman, D. F., and Enoka, R. M. Increase in heterogeneity of biceps brachii activation during isometric submaximal fatiguing contractions: a multichannel surface EMG study. *Journal of neurophysiology*, 111(5):984–90, 2014.

Tkach, D., Huang, H., and Kuiken, T. a. Study of stability of time-domain features for electromyographic pattern recognition. *Journal of Neuroengineering and Rehabilitation*, 7:21, 2010.

Tucker, K., Falla, D., Graven-Nielsen, T., and Farina, D. Electromyographic mapping of the erector spinae muscle with varying load and during sustained contraction. *Journal of Electromyography and Kinesiology*, 19(3):373–9, jun 2009.

Vaca Benitez, L. M., Tabie, M., Will, N., Schmidt, S., Jordan, M., and Kirchner, E. A. Exoskeleton technology in rehabilitation: Towards an EMG-based orthosis system for upper limb neuromotor rehabilitation. *Journal of Robotics*, 2013:13, 2013.

Valle, S., Li, W., and Qin, S. J. Selection of the Number of Principal Components: The Variance of the Reconstruction Error Criterion with a Comparison to Other Methods. *Industrial and Engineering Chemistry Research*, 38(11):4389–4401, 1999.

van Dijk, L., van der Sluis, C. K., van Dijk, H. W., Bongers, R. M., and Scheidt, R. Learning an EMG Controlled Game: Task-Specific Adaptations and Transfer. *PLOS ONE*, 11(8): e0160817, 2016.

Verikas, A., Vaiciukynas, E., Gelzinis, A., Parker, J., and Olsson, M. Electromyographic Patterns during Golf Swing: Activation Sequence Profiling and Prediction of Shot Effectiveness. *Sensors*, 16(5):592, 2016.

Vidovic, M. M.-C., Hwang, H.-J., Amsuss, S., Hahne, J. M., Farina, D., and Muller, K.-R. Improving the Robustness of Myoelectric Pattern Recognition for Upper Limb Prostheses by Covariate Shift Adaptation. *IEEE Transactions on Neural Systems and Rehabilitation Engineering*, 24(9):961–970, 2016.

Vieira, T. M. M., Merletti, R., and Mesin, L. Automatic segmentation of surface EMG images: Improving the estimation of neuromuscular activity. *Journal of Biomechanics*, 43(11):2149–58, 2010.

Wan, B., Xu, L., Ren, Y., Wang, L., Qiu, S., Liu, X., Liu, X., Qi, H., Ming, D., and Wang, W. Study on fatigue feature from forearm SEMG signal based on wavelet analysis. *2010 IEEE International Conference on Robotics and Biomimetics, ROBIO 2010*, pages 1229–1232, 2010.

Wang, Y., Li, J., and Li, Y. Measure for data partitioning in m x 2 cross-validation. *Pattern Recognition Letters*, 65:211–217, 2015.

Young, A. J., Hargrove, L. J., and Kuiken, T. A. The Effects of Electrode Size and Orientation on the Sensitivity of Myoelectric Pattern Recognition Systems to Electrode Shift. *IEEE Transactions on Biomedical Engineering*, 58(9):2537–2544, 2011.

Young, A. J., Hargrove, L. J., and Kuiken, T. a. Improving myoelectric pattern recognition robustness to electrode shift by changing interelectrode distance and electrode configuration. *IEEE Transactions on Biomedical Engineering*, 59(3):645–652, 2012.

Young, A. J., Smith, L. H., Rouse, E. J., and Hargrove, L. J. Classification of simultaneous movements using surface EMG pattern recognition. *IEEE Transactions on Biomedical Engineering*, 60(5):1250–1258, 2013.

Young, W. Spinal Cord Injury Levels & Classification, W M Keck Center for Collaborative Neuroscience.

Zhang, X. and Zhou, P. High-Density Myoelectric Pattern Recognition Toward Improved Stroke Rehabilitation. *IEEE Transactions on Biomedical Engineering*, 59(6):1649–1657, 2012.

Zimmer, C. and Sahle, S. Comparison of approaches for parameter estimation on stochastic models: Generic least squares versus specialized approaches. *Computational Biology and Chemistry*, 61:75–85, 2016.